Eur. Phys. J. Special Topics **226**, 365–371 (2017)

DOI: 10.1140/epjst/e2016-60182-y

THE EUROPEAN PHYSICAL JOURNAL SPECIAL TOPICS

Regular Article

Reducing low-frequency noise during reversible fluctuations

Ralph V. Chamberlin[a]

Department of Physics, Arizona State University, Tempe, AZ 85287-1504, USA

Received 19 June 2016 / Received in final form 24 September 2016
Published online 6 March 2017

Abstract. The noise from most materials exhibits a power-spectral density that tends to diverge as $S(f) \propto 1/f$ at low frequencies, f. A fundamental mechanism for this $1/f$ noise comes from the thermodynamics of small systems applied to reversible fluctuations of nanometer-sized regions inside bulk samples. Here this "nanothermodynamics" is used to derive a nonlinear correction to Boltzmann's factor. Specifically: Boltzmann's factor comes from the first-order (linear) derivative of entropy with respect to energy, whereas the nonlinear correction comes from higher-order terms. The nonlinear correction is applied to Monte Carlo simulations of small regions in the Ising model, yielding a low-frequency crossover to white noise that keeps the power-spectral density finite as $f \to 0$. It is shown that the low-frequency noise in the model is reduced by reducing the size of the regions.

Fluctuations of individual nanometer-sized systems can be measured using sophisticated techniques [1–8], and interpreted using modern fluctuation theorems [9–14]. Most of these fluctuation theorems are based on Boltzmann's factor, which assumes ideal thermal contact to an effectively infinite heat reservoir at a fixed temperature [15–17]. However even for bulk materials, several experimental techniques have shown that the primary response often involves independently relaxing, nanometer-sized regions that are uncorrelated with neighboring regions [18–24], with an effective local temperature that may temporarily fluctuate away from the infinite reservoir [25–30]. Nanothermodynamics provides the theoretical foundation for treating the thermal properties of individual small systems in a self-consistent manner, with a local thermal bath due to neighboring regions that are similarly small [31–34]. A common consequence is a nonlinear correction to Boltzmann's factor that yields non-Gaussian fluctuations that differ from those predicted by macroscopic statistical mechanics. A common result is that the thermal fluctuations exhibit noise with a power spectral density that varies as $\mathrm{S}(f) \sim 1/f$ over a wide range of frequencies, consistent with what is often measured in materials.

Thermal fluctuations exhibiting $1/f$-like noise were first reported in 1925 from measurements on early electron-tube amplifiers [35]. Similar $1/f$-like noise has since been found in most materials [36]; as well as in electronic, magnetic, and quantum devices [37–39]]; biological systems [40,41], and human perceptions [42,43].

[a] e-mail: ralph.chamberlin@asu.edu

Although no single model can explain all details in every system, such ubiquity suggests that $1/f$ noise involves a general principle that is not yet fully appreciated. Nanothermodynamics provides a common foundation for understanding $1/f$-like noise in many systems [44]. The key requirement is strict adherence to the laws of thermodynamics [31,34,45,46]. Specifically, non-extensive contributions to energy are accommodated using Hill's subdivision potential ε, and equilibrium fluctuations that decrease the entropy of the system are balanced by increasing the entropy of the surrounding sample. Another feature facilitates the statistics of indistinguishable particles, thereby avoiding Gibbs' paradox during equilibrium fluctuations. Here I focus on how nanothermodynamics is used to minimize the free energy in the fully-open generalized ensemble, thus allowing heterogeneous fluctuations inside bulk samples, which are ill-defined in standard thermodynamics.

Hill's subdivision potential can be understood by comparison to Gibbs' chemical potential, μ. In standard thermodynamics μ is an intensive parameter that comes from the first-order derivative of energy with respect to the number of particles N, whereas Hill's ε comes from higher-order derivatives, discrete-particle differences, and other non-extensive contributions to the energy of finite-sized systems. Note that some non-extensive contributions (e.g surface terms) can be added to the energy in an ad hoc fashion, but internal fluctuations that alter the total energy cannot be treated using standard thermodynamics. A fundamental thermodynamic equation for conservation of energy in magnetic systems is $\varepsilon = \overline{E}–TS–H\overline{M}–\mu\overline{N}$, adapted from Equation 10–3 in [31]. Here S is the entropy, T is temperature, and H is the external magnetic field; while the thermal-average properties are internal energy $\overline{E}$, magnetic moment $\overline{M}$, and particle number $\overline{N}$. Note that different properties are averaged in other ensembles, and that ε depends on the ensemble, as expected for small systems where fluctuations influence the total energy. Also note that the Gibbs-Duhem relation requires $\varepsilon \to 0$ as $N \to \infty$, because in standard thermodynamics E is assumed to be a linear homogenous function of S, M, and N. However, non-extensive contributions from internal fluctuations in heterogeneous systems must be included if total energy is to be conserved.

For simplicity I start with an ideal system of n non-interacting Ising-like particles ("spins"), each with alignment (σ_i) that may be up (+1) or down (–1). Although the Ising model was originally developed to describe ferromagnets, it is now a ubiquitous model for investigating the basic behavior of multi-particle systems. The net alignment of the system is $m = \sum_{i=1}^{n} \sigma_i$, where $-n \le m \le n$. The binomial coefficient gives the exact multiplicity of each alignment, $\Omega_{m,n} = n!/[{}^1\!/_2(n+m)]![{}^1\!/_2(n-m)]!$ Connection to thermodynamics is made through Boltzmann's entropy $S_{m,n} = k\ln(\Omega_{m,n})$, where k is Boltzmann's constant. The maximum entropy is $S_{0,n} = k\ln(\Omega_{0,n})$ with $\Omega_{0,n} = n!/[({}^1\!/_2 n)!]^2$. For non-interacting particles in zero field (where $\overline{E}$ =0), $\Omega_{0,n}$ also minimizes the Helmholtz free energy $F_{m,n} = \overline{E}–TS_{m,n}$. As discussed in chapter 11 of [31], using the change of variables $B = n$ and $N = {}^1\!/_2(n+m)$ this ideal Ising model is equivalent to the ideal lattice gas for the number of ways that N identical (indistinguishable) particles can be placed on B binding sites. In chapter 15 (pp. 203–205) Hill treats this ideal lattice gas using discrete difference equations with exact factorials, and shows that even the first-order thermal properties differ from those based on continuous degrees of freedom. Adapting his results to the ideal Ising model I obtain an internal field $h_{m,n} \equiv (F_{m+{}^1\!/_2,n} - F_{m-{}^1\!/_2,n}) = kT\ln[(n+m+1)/(n-m+1)]$ and chemical potential $\mu_{m,n} \equiv {}^1\!/_2[(F_{m+{}^1\!/_2,n+{}^1\!/_2} - F_{m-{}^1\!/_2,n-{}^1\!/_2}) + (F_{m-{}^1\!/_2,n+{}^1\!/_2} - F_{m+{}^1\!/_2,n-{}^1\!/_2}) = kT\ln[\sqrt{(n+1)^2 - m^2}/(2n+1)]$. Note that I use half-integer values for m and n to more-accurately define the differences around each integer [47], and to ensure that energy is symmetrical about $m = 0$, with $h_{0,n}$ =0. Also note that because $\overline{E} = 0$, both $h_{m,n}$ and $\mu_{m,n}$

come entirely from changes in entropy, due to a type of entropic force that is well-known for polymers [46,48,49]. Finally note that in the usual thermodynamic limit ($n \to \infty$) with $m \ll n$, the limiting values are $h_{m,n} = 0$ and $\mu_{m,n} = -kT\ln(2)$. For finite systems, however, the subdivision potential (similar to Equation (15–94) in [31]), from $\varepsilon_{m,n} = \overline{E} - TS_{m,n} - h_{m,n}m - \mu_{m,n}n$ with $\overline{E} = 0$, becomes

$$\frac{\varepsilon_{m,n}}{kT} = -\ln\left[\frac{n!}{(\frac{n+m}{2})!(\frac{n-m}{2})!}\left(\frac{n+m+1}{n-m+1}\right)^{m}\left(\frac{\sqrt{(n+1)^2-m^2}}{2n+1}\right)^{n}\right]. \qquad (1)$$

In chapter 10 (p. 101 of [31]) Hill shows how the subdivision potential depends on the ensemble. In the fully-open (μ,H,T) ensemble, which allows spontaneous fluctuations in m and n, thermal equilibrium is found by setting $\varepsilon = 0$ (see Eqs. (10–117)). This is analogous to $\mu = 0$ in the grand-canonical ensemble, where the number of modes (e.g. photons or phonons) must also fluctuate freely. In standard statistical mechanics, normal thermal fluctuations of extensive parameters vary proportional to the square root in the number of particles, $m \sim \sqrt{n}$. Specifically for the root-mean-squared average of m, neglecting the internal field so that the alignment probabilities are governed solely by the multiplicities, $m_{\text{rms}} = \sqrt{\sum_{m=-n}^{n} m^2\,\Omega_{m,n} / \sum_{-n}^{n}\Omega_{m,n}}$. Converting the summations to integrals over m, extending the limits to $\pm\infty$, and approximating the multiplicities by a Gaussian yields $m_{\text{rms}} = \sqrt{n}$. Using this m_{rms}, with equation (1) set to zero, yields a thermal-equilibrium system size of $\overline{n} \approx 11.07$. It is interesting to note that measurements on glycerol in thermal equilibrium above the glass transition find slowly-relaxing regions that contain about 10 molecules [23]. Given the simplistic model and assumptions used in deriving equation (1), such close quantitative agreement is undoubtedly fortuitous, but the idea that thermal equilibrium requires independent nanometer-sized regions is unique to nanothermodynamics. Indeed, although the model is for simple dipoles in zero external field ($H = 0$), there is an internal field from finite-size fluctuations that minimizes the free energy and reduces the net energy by an average amount $h_{\sqrt{\overline{n}},\overline{n}}\sqrt{\overline{n}} \approx 1.883kT$. The internal field could come from dipolar interactions not considered explicitly here, or from thermal motion that tends to randomize alignments as in the entropic model for polymers [49]. In standard thermodynamics, heterogeneous regions with non-extensive energies from thermal fluctuations are not allowed. Now I consider interacting particles ($\overline{E} \neq 0$), and non-Gaussian fluctuations in small regions that yield $1/f$-like noise.

Inside bulk samples, spontaneous fluctuations of m and n should be treated in the generalized (μ,H,T) ensemble, see pp. 96–99 in chapter 10 of [31]. Again thermal equilibrium is found by setting the subdivision potential to zero, $0 = \overline{E} - TS_{m,n} - h_{m,n}m - \mu_{m,n}n$. First assume that the fluctuations are reversible, so that this condition for thermal equilibrium is maintained. Next assume that fluctuations in m and n are independent, with significantly slower fluctuations in n, consistent with measurements [21–24]. Thus, alignment fluctuations will occur in regions of relatively constant size, so that the chemical potential will be averaged to a value that does not depend on instantaneous alignment, $\mu_{m,n} \to \mu_{\overline{m},n}$. Therefore, because m and n are assumed to be independent, the equation for thermal equilibrium can be separated into two parts: $\mu_{\overline{m},n} = \overline{E}/n$ and $h_{m,n} = -TS_{m,n}/m$. Again in zero external field, reversible fluctuations from $0 \to m$ require a nonlinear amount of internal work $h_{m,n}m = -TS_{m,n}$. The negative sign indicates that the internal field favors ferromagnetic alignment, even with no interactions. Thus for Monte Carlo simulations, the Metropolis algorithm governs changes in energy (ΔE), while the nonlinear correction accommodates

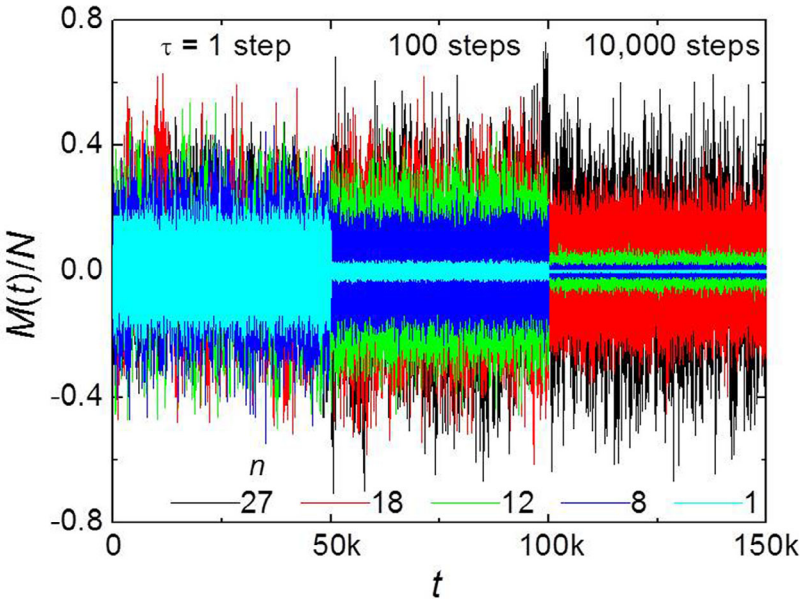

Fig. 1. Normalized magnetization as a function of time for averaging times of $\tau = 1$, 100, and 10,000 steps. All simulations are made on a system containing a total of $N = 216$ spins. Numbers of spins in each region (n) are: 27 (black), 18 (red), 12 (green), 8 (blue), and 1 (cyan), as given in the legend. Note that for smaller regions, averaging greatly reduces the amplitude of the fluctuations.

energy released due to reversible work ($-TS_{m,n}$):

$$\begin{aligned} e^{-\Delta E/kT} &> rand\,[0,1) \quad \text{Metropolis Algorithm, and} \\ e^{(S_{m,n}-S_{0,n})/k} &> rand\,[0,1) \quad \text{Nonlinear Correction.} \end{aligned} \tag{2}$$

I use Monte Carlo simulations of the Ising model to study thermal fluctuations that yield $1/f$ noise. A quadratic correction to Boltzmann's factor has been found to improve agreement between the Ising model and measured susceptibility of ferromagnetic materials and critical fluids [33], as well as nanometer-sized dynamical correlations in the structure of $LaMnO_3$ [46]. The correction to all orders (Eq. (2)) yields $1/f$-like noise over at least 8 orders of magnitude in frequency [44]. Here I study how the magnitude and frequency range of this $1/f$-like noise can be reduced by reducing the size of the regions.

I simulate the Ising model on a simple-cubic lattice having 6 spins on each side, for a total of $N = 216$ spins in the full sample. The interaction energy between nearest-neighbor spins is J, with periodic boundary conditions on all outside surfaces. The full sample is subdivided into smaller regions, each containing $n < N$ lattice sites. I record the alignment of the full sample as a function of time $M(t)$, which yields the net magnetization $M(t)/N$. For simulations over a wide dynamic range with a reasonable number of data points, I average $M(t)$ over various times τ, similar to how averaging is done in a measurement. Specifically, if $\tau = 1$ $M(t)$ is recorded every step, if $\tau = 10$ $M(t)$ is averaged over 10 steps before recording, up to $\tau = 10^6$ steps, with 2^{17} data points per simulation, yielding up to 1.31×10^{11} steps per simulation.

Figure 1 shows the net magnetization as a function of time from simulations having five different region sizes. Three different averaging times are taken from three sets of simulations, and separated into different time intervals along the time axis.

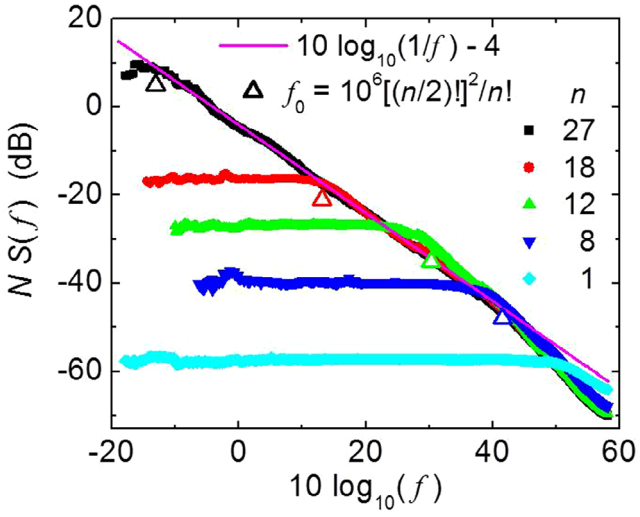

Fig. 2. Power spectral density of noise as a function of frequency on a log-log plot. Note that noise is multiplied by N to accommodate the size dependence of normal thermal fluctuations, and frequency is multiplied by 10 to match the dB scale. The magenta solid line shows exact $1/f$ behavior. Solid symbols come from simulations of systems with various region sizes: $n =$ 27 (black squares), 18 (red circles), 12 (green up-triangles), 8 (blue down-triangles), and 1 (cyan diamonds), also given in the legend. Open triangles, which mark the low-frequency end of the $1/f$-like regime, have frequencies inversely proportional to the maximum multiplicity of each region.

Note that for samples with small regions the fluctuations decrease with increasing averaging time, but the fluctuations remain large for samples with larger regions. Clearly, low-frequency fluctuations are reduced for samples with small regions.

Figure 2 shows the power spectral density as a function of frequency, $S(f)$, from simulations of $M(t)$ similar to those in Figure 1 but over much longer times for a wider frequency range. Magnetization as a function of time is converted to the power spectral density using a discrete Fourier transform: $S(f) = \left|\frac{1}{j}\sum_{t=0}^{j-1}[M(t)/N]\exp(-2\pi i f t/j)\right|^2$. The spectra are smoothed by linear regression using a sliding frequency range, where the spectral density at frequency f_1 comes from a linear least-squares fit to all data over the frequencies $-0.2 \leq 10\log_{10}(f/f_1) \leq 0.2$. Additional smoothing is achieved by simulating the system ~ 20 times using different initial conditions, but intrinsic noise is retained by analyzing each simulation separately before averaging.

The solid line in Figure 2 has a slope of –1 corresponding to exact $1/f$ behavior. The solid symbols in Figure 2 come from the simulations, showing $1/f$-like behavior over a frequency range that decreases with decreasing region size. The open triangles that mark the low-frequency knee of each $1/f$-like regime decrease inversely proportional to the maximum multiplicity of the spins in the region, $f_0 \sim 1/\Omega_{0,n} \approx 2^{-n}$. Consequently, the amplitude of noise at very low frequencies, below the $1/f$-like regime, increases exponentially with increasing n.

To summarize, a common mechanism for $1/f$ noise involves Hill's subdivision potential, ε. This ε is necessary to conserve total energy and maintain maximum entropy during equilibrium fluctuations. Here I focus on how $\varepsilon = 0$ minimizes the free energy in the fully-open generalized ensemble, which allows spontaneous fluctuations of nanometer-sized regions inside bulk samples with no artificial constraints. Ensuring

$\varepsilon = 0$ during reversible fluctuations yields a nonlinear correction to the Metropolis algorithm. Using this nonlinear correction for Monte Carlo simulations of the Ising model yields $1/f$-like noise over a range of frequencies. In this model, the size of the region governs the frequency range and maximum amplitude of the $1/f$ noise. Minimizing the region size minimizes the low-frequency noise.

I thank S. Abe, B.F. Davis, and G.H. Wolf for enlightening discusions. Most of the simulations utilized the A2C2 computing facility at Arizona State University. It is a pleasure to acknowledge Alberto Robledo for his kindness and creativity on the occasion of his 70^{th} birthday.

References

1. C.T. Rogers, R.A. Buhrman, Phys. Rev. Lett. **53**, 1272 (1984)
2. E. Vidal Russell, N.E. Israeloff, Nature **408**, 695 (2000)
3. D. Collin, F. Ritort, C. Jarzynski, S.B. Smith, I. Tinoco Jr, C. Bustamante, Nature **437**, 231 (2005)
4. S. Toyabe, T. Sagawa, M. Ueda, E. Muneyuki, M. Sano, Nat. Phys. **6**, 988 (2010)
5. J. Mehl, B. Lander, C. Bechinger, V. Blickle, U. Seifert, Phys. Rev. Lett. **108**, 220601 (2012)
6. A. Berut, A. Arkakelyan, A. Petrosyan, S. Ciliberto, R. Dillenschneider, E. Lutz, Nature **483**, 187 (2012)
7. J.V. Koski, T. Sagawa, O.P. Saira, Y. Yoon, A. Kutvonen, P. Solinas, M. Möttönen, T. Ala-Nissila, J.P. Pekola, Nat. Phys. **9**, 644 (2013)
8. G. Verley, M. Esposito, T. Willaert, C. Van den Broeck, Nat. Comm. **5**, 1 (2014)
9. G.E. Crooks, Phys. Rev. E **60**, 2721 (1999)
10. D.J. Evans, E.G.D. Cohen, G.P. Morriss, Phys. Rev. Lett. **71**, 2401 (1993)
11. G. Gallavotti, E.G.D. Cohen, Phys. Rev. Lett. **74**, 2694 (1995)
12. R. Kawai, J.M.R. Parrondo, C. Van den Broek, Phys. Rev. Lett. **98**, 080602 (2007)
13. S. Pressé, K. Ghosh, J. Lee, K.A. Dill, Rev. Mod. Phys. **85**, 1115 (2013)
14. U. Seifert, Rep. Prog. Phys. **75**, 1 (2012)
15. E.G.D. Cohen, D. Mauzerall, J. Stat. Mech: Theor. Exp. **2004**, P07006 (2004)
16. C. Jarzynski, J. Stat. Mech: Theor. Exp. **2004**, P09005 (2004)
17. R.P. Feynman, *Statistical Mechanics* (Westview Press, Boulder, CO, 1998)
18. E. Donth, J. Non-Cryst. Solids **53**, 325 (1982)
19. V.I. Yukalov, Phys. Rep. **208**, 395 (1991)
20. R. Böhmer, R.V. Chamberlin, G. Diezemann, B. Geil, A. Heuer, G. Hinze, S.C. Kuebler, R. Richert, B. Schiener, H. Sillescu, H.W. Spiess, U. Tracht, M. Wilhelm, J. Non-Cryst. Solids **235**, 1 (1998)
21. M.D. Ediger, Annu. Rev. Phys. Chem. **51**, 99 (2000)
22. R. Richert, J. Phys.: Condens. Matter **14**, R703 (2002)
23. S.A. Reinsberg, A. Heuer, B. Doliwa, H. Zimmermann, H.W. Spiess, J. Non-Cryst. Sol. **307**, 208 (2002)
24. L.J. Kaufman, Annu. Rev. Phys. Chem. **64**, 177 (2013)
25. M. Meissner, K. Spitzmann, Phys. Rev. Lett. **46**, 265 (1981)
26. P.K. Dixon, S.R. Nagel, Phys. Rev. Lett. **61**, 341 (1988)
27. R.V. Chamberlin, B. Schiener, R. Böhmer, MRS Bulletin **455**, 117 (1997)
28. R.V. Chamberlin, Phase Transitions **65**, 169 (1998)
29. R.V. Chamberlin, Phys. Rev. Lett. **83**, 5134 (1999)
30. R. Richert, S. Weinstein, Phys. Rev. Lett. **97**, 095703 (2006)
31. T.L. Hill, *Thermodynamics of Small Systems (Parts I and II)* (Dover, Mineola, NY, 1994)
32. R.V. Chamberlin, Nature **408**, 337 (2000)
33. R.V. Chamberlin, J.V. Vermaas, G.H. Wolf, Eur. Phys. J. B **71**, 1 (2009)

34. R.V. Chamberlin, Entropy **17**, 52 (2015)
35. J.B. Johnson, Phys. Rev. **26**, 71 (1925)
36. S. Kogan, *Electronic Noise and Fluctuations in Solids* (Cambridge University Press, Cambridge, 2008)
37. F. Yoshihara, K. Harrabi, A.O. Niskanen, Y. Nakamura, J.S. Tsai, Phys. Rev. Lett. **97**, 167001 (2006)
38. A.A. Balandin, Nature Nanotechnology **8**, 549 (2013)
39. E. Paladino, Y.M. Galperin, G. Falci, B.L. Altshuler, Rev. Mod. Phys. **86**, 361 (2014)
40. K.S. Nagapriya, A.K. Raychaudhuri, Phys. Rev. Lett. **96**, 038102 (2006)
41. R.M.M. Smeets, U.F. Keyser, N.H. Dekker, C. Dekker, Proc. Natl. Acad. Sci. U.S.A. **105**, 417 (2008)
42. J.P. Boon, Adv. Complex Syst. **13**, 155 (2010)
43. L.M. Ward, P.E. Greenwood, `http://www.scholarpedia.org/article/1/f)_noise`
44. R.V. Chamberlin, D.M. Nasir, Phys. Rev. E **90**, 012142 (2014)
45. R.V. Chamberlin, G.H. Wolf, Eur. Phys. J. B **67**, 495 (2009)
46. R.V. Chamberlin, Physica A **391**, 5384 (2012)
47. R.V. Chamberlin, B.F. Davis, Phys. Rev. E **88**, 042108 (2013)
48. H.M. James, E. Guth, J. Chem. Phys. **11**, 455 (1943)
49. R.P. Feynman, R.B. Leighton, M. Sands, *Lectures on Physics* (Pearson Addison Wesley, San Francisco, 2006), Vol. 1, p. 44